Bioorganic & Medicinal Chemistry Letters 26 (2016) 1869–1872

Contents lists available at ScienceDirect

Bioorganic & Medicinal Chemistry Letters

journal homepage: www.elsevier.com/locate/bmcl

Lead optimization of the VU0486321 series of $mGlu_1$ PAMs. Part 3. Engineering plasma stability by discovery and optimization of isoindolinone analogs

Pedro M. Garcia-Barrantes [a], Hyekyung P. Cho [a,b], Anna L. Blobaum [a], Colleen M. Niswender [a,b], P. Jeffrey Conn [a,b], Craig W. Lindsley [a,b,c,*]

[a] Vanderbilt Center for Neuroscience Drug Discovery, Vanderbilt University Medical Center, Nashville, TN 37232, USA
[b] Department of Pharmacology, Vanderbilt University School of Medicine, Nashville, TN 37232, USA
[c] Department of Chemistry, Vanderbilt University, Nashville, TN 37232, USA

ARTICLE INFO

Article history:
Received 15 February 2016
Revised 8 March 2016
Accepted 9 March 2016
Available online 10 March 2016

Keywords:
$mGlu_1$
Metabotropic glutamate receptor
Positive allosteric modulator (PAM)
Schizophrenia
Structure–activity relationship (SAR)

ABSTRACT

This Letter describes the further lead optimization of the VU0486321 series of $mGlu_1$ positive allosteric modulators (PAMs), focused on addressing the recurrent issue of plasma instability of the phthalimide moiety. Here, we evaluated a number of phthalimide bioisosteres, and ultimately identified isoindolinones as the ideal replacement that effectively address plasma instability, while maintaining acceptable $mGlu_1$ PAM potency, DMPK profile, CNS penetration and mGluR selectivity.

Recent genetic data implicating *GRM1* in schizophrenia[1–3] and studies showing that the adverse affect liabilities of group I metabotropic glutamate receptors (mGluRs) is mediated by $mGlu_5$ and not $mGlu_1$,[4] have rekindled interest in the development of $mGlu_1$ positive allosteric modulators (PAMs).[3–6] However, early $mGlu_1$ PAMs lacked the DMPK profiles to serve as robust in vivo tool compounds (Fig. 1).[7]

In response, our lab has focused efforts on developing novel $mGlu_1$ PAMs,[3–6] with an intent to discover the ideal in vivo tool compound to then validate the target for multiple neuropsychiatric disorders. Within the phthalimide-based VU0486321 series of $mGlu_1$ PAMs, most optimization parameters could be effectively addressed (potency, disposition, CNS penetration), except for reoccurring and variable in vitro plasma instability due to hydrolysis of the phthalimide moiety.[3–6,8] In this Letter, we explore phthalimide biosiosteres and other replacements, ultimately identifying isoindolinones as the ideal substitute, and the discovery of VU0487351, a potent, selective, CNS penetrant and stable $mGlu_1$ PAM tool compound.

The optimization plan targeted expansion of the phthalimide moiety, saturated analogs and sequential deletion of carbonyl moieties to provide isoindolionones and isoindolines (Fig. 2) to deliver diverse analogs **6**. The chemistry required is straight forward, as shown in Scheme 1, requiring only three steps from commercial materials to access final compounds **9**, **13** and **16**. Nucleophilic aromatic substitution between **7** and different amines produced intermediates **8**, which where hydrogenated and submitted to amide coupling with 3-methyl-2-furoic acid to give analogs **9**. Functionalized *p*-amino nitroarenes/heteroarenes **10** were condensed with various anhydrides to afford analogs **11**. The nitro group was reduced to the aniline **12** via hydrogenation conditions, and final analogs **6** were afforded by standard amide coupling conditions with a diverse array of heterocyclic carboxylic acids to provide analogs **13**. Alternatively, **7** could be employed to displace benzylic bromides **14**, which upon heating formed the γ-lactams **15**. Then, nitro reduction and acylation would yield the diversely functionalized isoindolinones **16**.[9]

Initially, we evaluated analogs of **3**, and the SAR was intriguing. Expansion of the phthalimide moiety to an isoquinoline dione **17** (Fig. 2) afforded a potent $mGlu_1$ PAM (EC_{50} = 242 nM, pEC_{50} = 6.65 ± 0.09, 105% Glu Max)[10] with a clean CYP profile, but high intrinsic clearance (13.5 mL/min/kg and 54 mL/min/kg for human and rat, respectively) and was found to be unstable in both rat and human plasma. Further expansion to the seven-membered benzo[*d*]azepine core **18**, led to a significant loss of activity

* Corresponding author.
E-mail address: craig.lindsley@vanderbilt.edu (C.W. Lindsley).

http://dx.doi.org/10.1016/j.bmcl.2016.03.031
0960-894X/

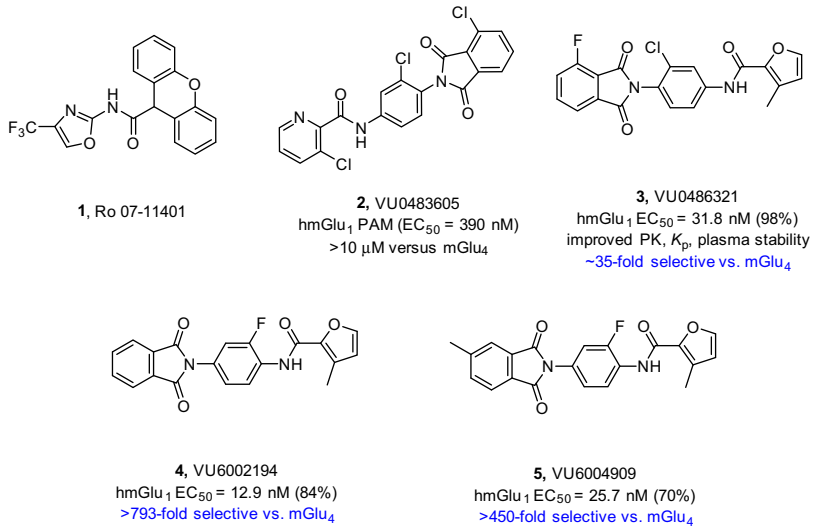

Figure 1. Structures of representative $mGlu_1$ PAMs **1–5**.

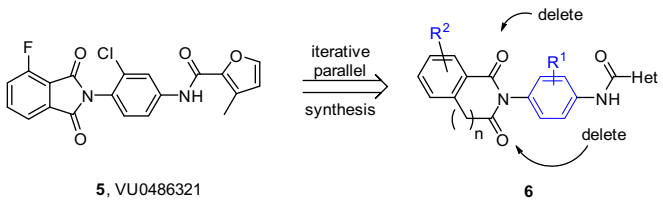

Figure 2. Chemical optimization plan to replace the phthalimide moiety of **5** with novel analogs **6**.

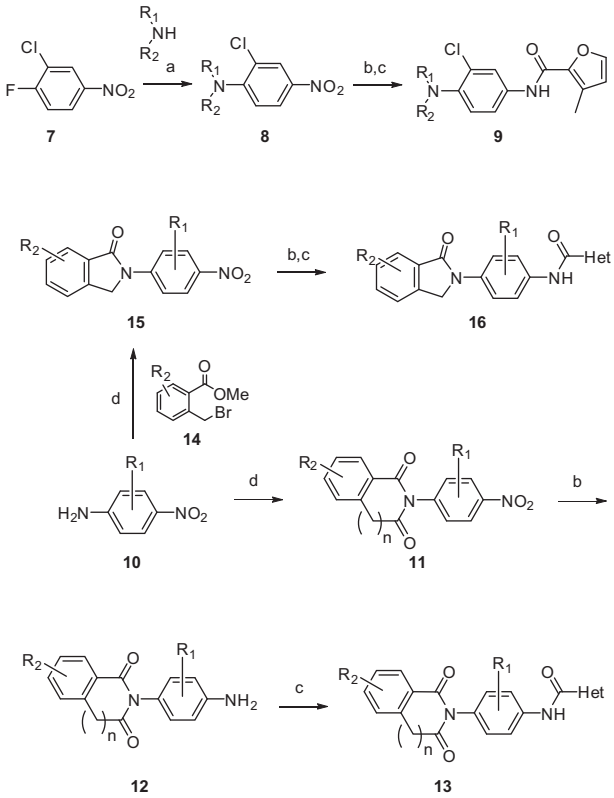

Scheme 1. Reagents and conditions: (a) K_2CO_3, ACN, 60 °C, 43–89%, (b) H_2, Pd/C, EtOH, rt, 94–99%; (c) heterocyclic carboxylic acids, HATU, DCM, rt, 39–98%; (d) aryl anhydrides, AcOH, reflux, 64–94%; (e) K_2CO_3, DMF, μW, 150 °C, 15 min, 29–92%.

(EC_{50} = 3.5 μM, pEC_{50} = 5.44 ± 0.08, 95% Glu Max). Interestingly, a 3,4-dihydroquinolinone congener **19**, was a modest $mGlu_1$ PAM (EC_{50} = 1.29 μM, pEC_{50} = 5.88 ± 0.09, 107% Glu Max) with supra-hepatic clearance; however, **19** was stable in human and rat plasma, and suggested lactams may be productive in engendering plasma stability (Fig. 3).

Based on these data, we then explored a diverse array of phthalimide replacements **20**, with varying degrees of success (Table 1). Representative examples include **20a** and **20b**, the direct, saturated (both *cis*- and *trans*-isomers) of **3**, which proved to be inactive. The hydrolyzed product of **3**, **20c**, was synthesized and found to be active (EC_{50} = 930 nM, pEC_{50} = 6.03 ± 0.14, 108% Glu Max); however, **20c** was not CNS penetrant and displayed poor disposition, yet an 'active' in vitro metabolite. Other benzoates, with diverse functional groups in place of the carboxylic acid were all inactive. Isoindolinone **20e** was active, but the regioisomeric congener **20g** was inactive, and both regioisomeric isoindolines, **20f** and **20h** were active. **20l**, a regiosiomer of **19** was potent (EC_{50} = 780 nM, pEC_{50} = 6.11 ± 0.12, 94% Glu Max) as well. Profiling of all the active analogs **20** in our in vitro DMPK assays quickly led us to focus on the isoindolinone **17e** (EC_{50} = 3.72 μM, pEC_{50} = 5.43 ± 0.19, 91% Glu Max), as it displayed complete stability in rat and human liver microsomes with low intrinsic clearance. Now, the focus was to improve $mGlu_1$ PAM potency.

For the next iteration of parallel synthesis, we surveyed functionalized isoindolinone congeners **21**, of the $mGlu_1$ PAM **3** (Table 2). Gratifyingly, substituents on the isoindolinone phenyl ring increased potency by >10-fold in some cases, providing $mGlu_1$ PAMs with nanomolar potency.

Evaluation of analogs **21** in our in vitro and in vivo battery of DMPK assays quickly identified **21a** (VU0487351),[3–6,11] as an exceptional compound. First, and in contrast to **3**–**5**, **21a** was hydrolytically stable in rat and human liver microsomes and displayed moderate intrinsic clearance (rat CL_{hep} 54.1 mL/min/kg and human CL_{hep} 8.53 mL/min/kg). Moreover, **21a** had a clean CYP profile (IC_{50}s > 30 μM against 3A4, 1A2, 2C9 and 2D6), was inactive at $mGlu_4$ (EC_{50} > 10 μM) and was found to be highly CNS penetrant (K_p = 1.36, C_n plasma 193 nM and C_n brain 269 nM). In vivo, **21a** displayed favorable rat PK, with a low clearance (CL_p 11.1 mL/min/kg), high distribution volume (V_D 3.36 L/kg) and good half-life ($t_{1/2}$ = 93 min, MRT = 302 min). Therefore, the isoindolinone moiety solved the plasma instability issue, as well as affording a favorable in vitro and in vivo DMPK profile. The only blemish for **21a** was high protein binding (>99% in human and

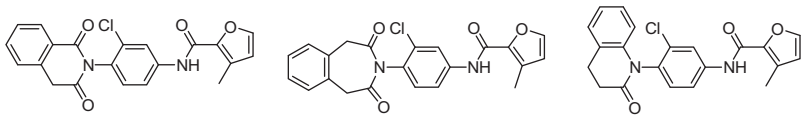

17 18 19

Figure 3. Homologated analogs **14**–**16** of **3** that retained $mGlu_1$ PAM activity.

Table 1
Structures and activities for analogs **20**

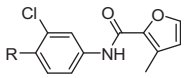

20

Cpd	Het	$hmGlu_1$ EC_{50} (μM)[a] [% Glu Max ± SEM]	$mGlu_1$ pEC_{50} (±SEM)
20a	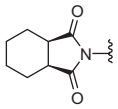	>10 [—]	>5
20b	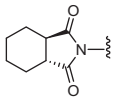	>10 [—]	>5
20c	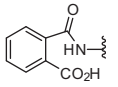	0.93 [108 ± 7]	6.03 ± 0.14
20d	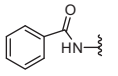	>10 [-]	>5
20e	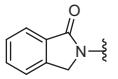	3.72 [91 ± 9]	5.43 ± 0.19
20f	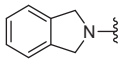	1.76 [95 ± 23]	5.75 ± 0.43
20g	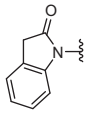	>10 [—]	>5
20h		5.71 [82 ± 8]	5.24 ± 0.14
20i	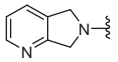	9.55 [78 ± 2]	5.02 ± 0.09
20j		3.62 [99 ± 9]	5.44 ± 0.14
20k		2.61 [93 ± 4]	5.58 ± 0.07
20l	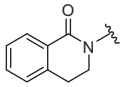	0.781 [94 ± 4]	6.11 ± 0.12
20m	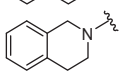	2.47 [107 ± 5]	5.88 ± 0.09

[a] Calcium mobilization $mGlu_1$ assays, values are average of three ($n = 3$) independent experiments performed in triplicate.

rat plasma, as well as rat brain homogenate binding), which was true for all analogs **21** ($f_u < 0.01$). Therefore, we elected to pursue a matrix library strategy to identify new isoindolinone-based $mGlu_1$ PAMs that maintained the overall profile of **21a**, while improving fraction unbound.

Table 2
Structures and activities for analogs **21**

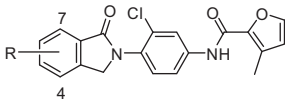

21

Cpd	R	$hmGlu_1$ EC_{50} (μM)[a] [% Glu Max ± SEM]	$mGlu_1$ pEC_{50} (±SEM)
21a	4-Cl	0.211 [88 ± 4]	6.75 ± 0.07
21b	5-Cl	>10 [58 ± 1]	>5
21c	7-Cl	0.484 [108 ± 4]	6.31 ± 0.1
21d	4-Me	1.07 [89 ± 3]	5.96 ± 0.09
21e	4-F	0.878 [82 ± 4]	6.05 ± 0.11
21f	4-Br	0.391 [99 ± 4]	6.41 ± 0.10
21g	4-CF_3	1.13 [105 ± 5]	5.94 ± 0.09
21h	4-CN	2.09 [107 ± 9]	5.67 ± 0.17
21i	4-OMe	>10 [—]	>5
21j	4-Aza	>10 [—]	>5
21k	7-Aza	>10 [—]	>5
21l	4,7-Aza	>10 [—]	>5
21m	3,3-diMe	6.93 [76 ± 3]	5.15 ± 0.09

[a] Calcium mobilization $mGlu_1$ assays, values are average of three ($n = 3$) independent experiments performed in triplicate.

Analogs **22** surveyed SAR for three regions: the central phenyl core, alternative heterocyclic amides and substitutions on the isoindolinone phenyl ring (Table 3). The removal of the hydrogen in the central ring (**22a**–**c**) led to a similar SAR tendency as the 2-Cl analogs, with **22b** having a comparable potency to **21a**, suggesting that an asymmetric substitution pattern in the central ring is not necessary. Other substitutions, such as 2,3-dichloro (**22d**–**f**) and 3-fluoro (**22g**–**i**) caused a dramatic loss in potency. This trend shows how variable and steep the SAR can be in this scaffold, as the 3-fluoro substitution has been an excellent modification to achieve potent and selective $mGlu_1$ PAM activity in our phthalimide scaffold. As we assessed the replacement of the furan with different heterocycles in the isoindolinone scaffold, a substantial loss in potency was found when using 3-substituted picolinamides, and only the 4-Cl substituted **22h** and **22k** (direct comparators to **21a**) maintained $mGlu_1$ PAM potency of around 1 μM; while in the thiazole (**22p**–**r**) congeners the 4-Cl substituted (**22q**) was most potent of the group ($EC_{50} = 950$ nM). However, these attempts to engender improved free fraction in the isoindolinone series failed, and SAR was steep.

In conclusion, the continued optimization of the VU0486321 series of $mGlu_1$ PAMs led us to pursue alternatives for the phthalimide moiety, plagued with unpredictable plasma instability issues. Here we identified isoindolinones as biosiosteres for the phthalimide group. $mGlu_1$ PAMs such as **21a**, that retained $mGlu_1$ PAM potency and mGluR selectivity, while also affording plasma stability, attractive in vitro and in vivo PK profiles and high CNS penetration ($K_p = 1.36$). Together, with VU0487351 (**21a**) and VU6004909 (**5**), the field now has $mGlu_1$ PAMs that can serve as robust in vivo tool compounds to further dissect the therapeutic potential of selective $mGlu_1$ activation.

Table 3
Structures and activities for analogs **22**

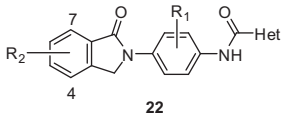

22

Cpd	R^1	R^2	Het	$hmGlu_1$ EC_{50} (μM)[a] [% Glu Max ± SEM]	$mGlu_1$ pEC_{50} (±SEM)
22a	H	H		1.56 [94 ± 12]	5.81 ± 0.31
22b	H	4-Cl		0.245 [99 ± 3]	6.61 ± 0.11
22c	H	7-Cl		0.353 [101 ± 3]	6.45 ± 0.11
22d	2,3-diCl	H		>10 [—]	>5
22e	2,3-diCl	4-Cl		>10 [—]	>5
22f	2,3-diCl	7-Cl		6.52 [81 ± 6]	5.18 ± 0.09
22g	3-F	H		>10 [—]	>5
22h	3-F	4-Cl		1.26 [86 ± 6]	5.90 ± 0.15
22i	3-F	7-Cl		>10 [—]	>5
22j	2-Cl	H		>10 [—]	>5
22k	2-Cl	4-Cl		1.36 [97 ± 6]	5.84 ± 0.14
22l	2-Cl	7-Cl		>10 [78 ± 2]	>5
22m	2-Cl	H		>10 [—]	>5
22n	2-Cl	4-Cl		1.27 [93 ± 5]	5.89 ± 0.12
22o	2-Cl	7-Cl		>10 [51 ± 3]	>5
22p	2-Cl	H		>10 [33 ± 6]	>5
22q	2-Cl	4-Cl		0.954 [66 ± 4]	6.02 ± 0.12
22r	2-Cl	7-Cl		4.69 [69 ± 2]	5.32 ± 0.73

[a] Calcium mobilization $mGlu_1$ assays, values are average of three ($n = 3$) independent experiments performed in triplicate.

Acknowledgments

We thank William K. Warren, Jr. and the William K. Warren Foundation who funded the William K. Warren, Jr. Chair in Medicine (to C.W.L.). P.M.G. would like to acknowledge the VISP program for its support. This work was funded by the William K. Warren, Jr. Chair in Medicine and the NIH (U54MH084659).

References and notes

1. Frank, R. A. W.; McRae, A. F.; Pocklington, A. J.; van de Lagemaat, L. N.; Navarro, P.; Croning, M. D. R.; Komiyama, N. H.; Bradley, S. J.; Challiss, R. A. J.; Armstrong, J. D.; Finn, R. D.; Malloy, M. P.; MacLean, A. W.; Harris, S. E.; Starr, J. M.; Bhaskar, S. S.; Howard, E. K.; Hunt, S. E.; Coffey, A. J.; Raganath, V.; Deloukas, P.; Rogers, J.; Muir, W. J.; Deary, I. J.; Blackwood, D. H.; Visscher, P. M.; Grant, S. G. N. *PLoS One* **2011**, *6* e19011.
2. Ayoub, M. A.; Angelicheva, D.; Vile, D.; Chandler, D.; Morar, B.; Cavanaugh, J. A.; Visscher, P. M.; Jablensky, A.; Pfleger, K. D. G.; Kalaydijeva, L. *PLoS One* **2012**, *7* e32849.
3. Cho, H. P.; Garcia-Barrantes, P. M.; Brogan, J. T.; Hopkins, C. R.; Niswender, C. M.; Rodriguez, A. L.; Venable, D.; Morrison, R. D.; Bubser, M.; Daniels, J. S.; Jones, C. K.; Conn, P. J.; Lindsley, C. W. *ACS Chem. Biol.* **2014**, *9*, 2334.
4. Garcia-Barrantes, P. M.; Cho, H. P.; Niswender, C. M.; Byers, F. W.; Locuson, C. W.; Blobaum, A. L.; Xiang, Z.; Rook, J. M.; Conn, P. J.; Lindsley, C. W. *J. Med. Chem.* **2015**, *58*. 7959–7571.
5. Garcia-Barrantes, P. M.; Cho, H. P.; Niswender, C. M.; Blobaum, A. L.; Conn, P. J.; Lindsley, C. W. *Bioorg. Med. Chem. Lett.* **2015**, *25*, 5107.
6. Garcia-Barrantes, P. M.; Cho, H. P.; Metts, A. M.; Blobaum, A. L.; Niswender, C. M.; Conn, P. J.; Lindsley, C. W. *Bioorg. Med. Chem. Lett.* **2016**, *26*, 751.
7. Vieira, E.; Huwyler, J.; Jolidon, S.; Knoflach, F.; Mutel, V.; Wichmann, J. *Bioorg. Med. Chem. Lett.* **2009**, *19*, 1666.
8. Jones, C. K.; Engers, D. W.; Thompson, A. D.; Field, J. R.; Blobaum, A. L.; Lindsley, S. R.; Zhou, Y.; Gogliotti, R. D.; Jadhav, S.; Zamorano, R.; Daniels, J. S.; Morrison, R.; Weaver, C. D.; Conn, P. J.; Lindsley, C. W.; Niswender, C. M.; Hopkins, C. R. *J. Med. Chem.* **2011**, *54*, 7639.
9. **Representative experimental (21a, VU0487351).** *N-(3-Chloro-4-(4-chloro-1-oxoisoindolin-2-yl)phenyl)-3-methylfuran-2-carboxamide* (**21a**): In a microwave vial, *N*-(4-amino-3-chlorophenyl)-3-methylfuran-2-carboxamide (preparation described in Ref. 4) (100 mg, 0.399 mmol) and K_2CO_3 (110 mg, 0.798 mmol) were weighted an dissolved in DMF (2 mL). The reaction was stirred for 10 min at room temperature followed by addition of 2-(bromomethyl)-3-chlorobenzoate (126 mg, 0.479 mmol). The reaction was heated in a microwave reactor for 15 min at 150 °C. The reaction was worked up by addition of water and successive extractions with DCM. The organic phases were combined and filtered through a phase separator. Volatiles were evaporated in vacuo and the crude was purified by trituration with cold MeOH. A cream solid was obtained (84.8 mg, 53%). ^{1}H NMR (400.1 MHz, $CDCl_3$) δ (ppm): 8.16 (1H, s), 8.02 (1H, d, J = 2.3 Hz), 7.87 (1H, J = 7.4 Hz), 7.59 (2H, m), 7.51 (1H, t, J = 7.7 Hz), 7.38 (2H, m), 6.42 (1H), 4.78 (2H, s), 2.47 (3H, s). ^{13}C NMR (100.6 MHz, $CDCl_3$) δ (ppm): 167.3, 157.2, 142.8, 141.4, 139.8, 138.6, 133.9, 133.1, 131.9, 130.7, 130.1, 129.9, 129.8, 129.2, 122.8, 121.1, 118.7, 116.0, 51.4, 11.2.
10. *In vitro molecular pharmacology*. Tetracycline-tested fetal bovine serum (FBS) was purchased from Atlanta Biologicals (Lawrenceville, GA), and all other tissue culture reagents and Fluo-4-acetoxymethylester (Fluo-4-AM) were purchased from Life Technologies (Carlsbad, CA). Tetracycline hydrochloride (Sigma), L-glutamic acid (Tocris, Minneapolis, MN), and (*S*)-3,5-dihydroxy phenylglycine (DHPG) (Abcam, Cambridge, MA). EZ-Link Sulfo-NHS-SS-Biotin and NeutrAvidin agarose beads (Pierce Biotechnology, Rockford, IL). Tetracycline-inducible human $mGlu_1$ WT-T-REx™-293 cells (Wu et al., Science 2014) were cultured at 37 °C in Dulbecco's Modified Eagle Medium (DMEM) growth medium containing 10% Tet-tested FBS, 2 mM L-glutamine, 20 mM HEPES, 0.1 mM non-essential amino acids, 1 mM sodium pyruvate, antibiotic/antimycotic, 100 μg/mL hygromycin and 5 μg/mL blasticidin in the presence of 5% CO_2. To determine the potency of $mGlu_1$ PAMs in calcium assays, Ca flux was measured as previously described in *ACS Chem. Biol.* **2014**, *9*, 2334. Briefly, the day before the assay, human $mGlu_1$ WT-T-REx™-293 cells were plated in black-walled, clear-bottomed, poly-D-lysine coated 96-well plates at 80,000 cells/100 μL assay medium (DMEM supplemented with 10% dialyzed FBS, 20 mM HEPES, and 1 mM sodium pyruvate) containing 50 ng/mL of tetracycline to induce $mGlu_1$ expression. The next day, media was removed and the cells were incubated with 50 μL of 1.15 μM Fluo-4 AM dye solution prepared in assay buffer (buffer (Hank's balanced salt solution, 20 mM HEPES, and 2.5 mM probenecid) for 45 min at 37 °C, the dye was removed and replaced with 45 μL of assay buffer. Then, calcium flux was measured using Flexstation II (Molecular Devices, Sunnyvale, CA). Compounds serially diluted at half log concentrations in DMSO were further diluted in assay buffer. The compounds or DMSO vehicle were added to cells and incubated for 2.5 min and an EC_{20} concentration of glutamate was added and incubated for 1 min. An EC_{max} concentration of glutamate was also added to cells that were incubated with DMSO vehicle to accurately calculate the EC_{20} calcium response. Data were normalized by subtracting the basal florescent peak before EC_{20} agonist addition from the maximal peak elicited by EC_{20} agonist and PAMs. Using GraphPad Prism 5.0, the concentration response curves were generated and the potencies of the $mGlu_1$ PAMs were determined.
11. Gentry, P. R.; Kokubo, M.; Bridges, T. M.; Byun, N.; Cho, H. P.; Smith, E.; Hodder, P. S.; Niswender, C. M.; Daniels, J. S.; Conn, P. J.; Lindsley, C. W.; Wood, M. R. *J. Med. Chem.* **2014**, *57*, 7804.